

Optimal Synthesis for Nonholonomic Vehicles With Constrained Side Sensors

Paolo Salaris^{*}, Lucia Pallottino^{*} and Antonio Bicchi^{* †}

February 14, 2011

Abstract

We present a complete characterization of shortest paths to a goal position for a vehicle with unicycle kinematics and a limited range sensor, constantly keeping a given landmark in sight. Previous work on this subject studied the optimal paths in case of a frontal, symmetrically limited Field-Of-View (FOV). In this paper we provide a generalization to the case of arbitrary FOVs, including the case that the direction of motion is not an axis of symmetry for the FOV, and even that it is not contained in the FOV. The provided solution is of particular relevance to applications using side-scanning, such as e.g. in underwater sonar-based surveying and navigation.

1 Introduction

In several mobile robot applications, a vehicle with nonholonomic kinematics of the unicycle type, equipped with a limited range sensor systems, has to reach a target while keeping some environment landmark in sight. For example, in the Visual-Based control field the vehicle usually has an on-board monocular camera with limited Field-Of-View (FOV) and, subject to nonholonomic constraints on its motion, must move maintaining in sight one or more specified features of the environment. On the other hand, in the field of underwater surveying and navigation, a common task for Autonomous Underwater Vehi-

cles (AUV) equipped with side sonar scanners is to detect and recognize objects (mines, wrecks or archeological find, etc.) on the sea bed (see e.g. [8, 10]). Side-scan sonar is a category of sonar systems that is used to efficiently create an image of large areas of the sea. Therefore, in order to recognize objects AUVs must move keeping them inside the limited range of the sensor.

Motivated by those application, in this paper we propose the study of optimal (shortest) paths for a nonholonomic vehicle moving in a plane to reach a target position while making so that a given landmark fixed in the plane is kept inside a planar cone moving with the robot.

The literature of optimal (shortest) paths stems mainly from the seminal work on unicycle vehicles with a bounded turning radius by Dubins [9]. Dubins has characterized the finite family of optimal paths for the particular vehicle while a complete optimal control synthesis for this problem has been reported in [4]. Later on, a similar problem with the car moving both forward and backward has been solved with different approaches in [11], [15]. In particular, in [14] the optimal control synthesis for the Reeds&Shepp car has been provided. Minimum wheel rotation paths in for differential-drive robots have been considered in [6]. More recently, also the problem of determining minimum time trajectory has been taken into account in [16], [1] and [7] for particular classes of robots, e.g. latter is on underwater robots. Finally, previous works on the same subject of this paper ([13], [12], [2]) have studied the optimal paths in case of a vehicle with a limited on-board camera but only with a symmetric FOV with respect to the forward direction of the robot. In this paper, we present a more general synthesis of shortest paths in case of side sensor systems, like side sonar scanners on UAVs, where the forward direction is not neces-

^{*}This work was supported by E.C. contracts n.224428 CHAT, n.224053 CONET (Cooperating Objects Network of Excellence), n. 257462 HYCON2 (Network of Excellence) and n.2577649 Planet.

[†]* The Interdept. Research Center “Enrico Piaggio”, University of Pisa, via Diotallevi 2, 56100 Pisa, Italy. paolo.salaris,l.pallottino,bicchi@ing.unipi.it

sarily included inside the sensor range modeled as a cone centered on the vehicle. The impracticability of paths that point straight to the feature lead to a more complex analysis of the reduction to a finite and sufficient family of optimal paths by excluding particular types of path.

In the rest of the paper, we provide a complete optimal synthesis for the problem, i.e., a finite language of optimal control words (at most 15 words, depending on orientation of the sensor with respect to the forward direction), and a global partition of the motion plane induced by shortest paths, such that a word in the optimal language is univocally associated to a region and completely describes the constrained shortest path from any starting point in that region to the goal point.

2 Problem Definition

Consider a vehicle moving on a plane where a right-handed reference frame $\langle W \rangle$ is defined with origin in O_W and axes X_W, Z_W . The configuration of the vehicle is described by $\xi(t) = (x(t), z(t), \theta(t))$, where $(x(t), z(t))$ is the position in $\langle W \rangle$ of a reference point in the vehicle, and $\theta(t)$ is the vehicle heading with respect to the X_W axis (see fig. 1). We assume that the dynamics of the vehicle are negligible, and that the forward and angular velocities, $v(t)$ and $\omega(t)$ respectively, are the control inputs to the kinematic model. Choosing polar coordinates for the vehicle $\eta = [\rho \ \psi \ \beta]^T$ (see fig. 1), the kinematic model of the unicycle-like robot is

$$\begin{bmatrix} \dot{\rho} \\ \dot{\psi} \\ \dot{\beta} \end{bmatrix} = \begin{bmatrix} -\cos\beta & 0 \\ \frac{\sin\beta}{\rho} & 0 \\ \frac{\sin\beta}{\rho} & -1 \end{bmatrix} \begin{bmatrix} v \\ \omega \end{bmatrix}. \quad (1)$$

We consider vehicles with bounded velocities which can turn on the spot. In other words, we assume

$$(v, \omega) \in U, \quad (2)$$

with U a compact and convex subset of \mathbb{R}^2 , containing the origin in its interior.

The vehicle is equipped with a rigidly fixed sensor system with a reference frame $\langle C \rangle = \{O_c, X_c, Y_c, Z_c\}$ such that the center O_c corresponds to the robot's center $[x(t), z(t)]^T$ and the forward sensor axis Z_c forms an angle Γ w.r.t the robot's forward direction. Moreover, let δ be

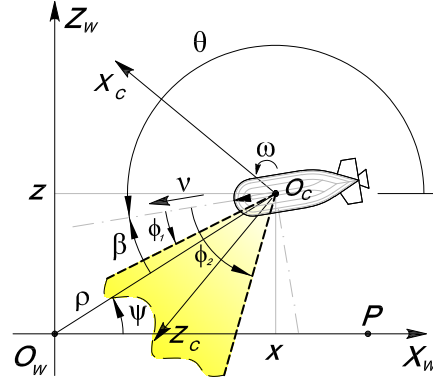


Figure 1: Autonomous vehicle and systems coordinates. The vehicle's task is to reach P while keeping O_W within a limited sensor range modelled as a planar cone (highlighted in color).

the characteristic angle of the cone characterizing the limited Sensor Range (SR) and let us consider the most interesting problem in which $\delta \leq \pi/2$. Without loss of generality, we will consider $0 \leq \Gamma \leq \frac{\pi}{2}$, so that, when $\Gamma = 0$ the Z_c axis is aligned with the robot's forward direction (i.e., the particular case solved in [13]), whereas, when $\Gamma = \frac{\pi}{2}$, is aligned with the axle direction. Consider $\phi_1 = \Gamma - \frac{\delta}{2}$ and $\phi_2 = \Gamma + \frac{\delta}{2}$ the angles between the robot's forward direction and the right or left sensor's border w.r.t. Z_c axis, respectively. The restriction on $0 \leq \Gamma = \frac{\phi_1 + \phi_2}{2} \leq \frac{\pi}{2}$ will be removed at the end of this paper, and an easy procedure to obtain the subdivision for any value of Γ will be given.

Without loss of generality, we consider the position of the robot target point P to lay on the X_W axis, with coordinates $(\rho, \psi) = (\rho_P, 0)$. We also assume that the feature to be kept within the SR is placed on the axis through the origin O_W and perpendicular to the plane of motion. We consider a planar SR with characteristic angle $\delta = |\phi_2 - \phi_1|$, which generates the constraints

$$\beta - \phi_1 \geq 0, \quad (3)$$

$$\beta - \phi_2 \leq 0. \quad (4)$$

Note that we place no restrictions on the vertical dimension of the sensor. Therefore, the height of the feature on the motion plane, which corresponds to its Y_c coordinate in the sensor frame $\langle C \rangle$, is irrelevant to our problem.

Hence, for our purposes, it is necessary to know only the projection of the feature on the motion plane, i.e., O_W .

The goal of this paper is to determine, for any point $Q \in \mathbb{R}^2$ in the robot space, the shortest path from Q to P such that the feature is maintained in the SR. In other words, we want to minimize the length of the path covered by the center of the vehicle under the *feasibility constraints* (1), (2), (3), and (4).

From the theory of optimal control with state and control constraints (see [3]) it is possible to show that, when constraints (3) and (4) are not active, extremals curves, i.e., curves that satisfy necessary conditions for optimality, are straight lines (denoted by symbol S) and rotation on the spot (denoted by symbol $*$). On the other hand, when constraints (3) and (4) are active, the corresponding extremal maneuvers are two logarithmic spirals with characteristic angles ϕ_1 and ϕ_2 denoted by T_1 and T_2 , respectively (see [13] for details).

Logarithmic spiral T with characteristic angle $\phi > 0$ ($\phi < 0$) rotates counterclockwise (clockwise) around the feature. We refer to counterclockwise and clockwise spirals as *Left* and *Right*, and by symbols T^L and T^R , respectively. The adjectives “left” and “right” indicate the half-plane where the spiral starts for an on-board observer aiming at the feature.

Notice that, for $\phi_2 = \pi/2$ the left sensor border is aligned with the axle direction and the spiral T_2 becomes a circle centered in O_W (denoted by C), whereas for $\phi_1 = 0$ the right sensor border is aligned with the direction of motion and T_1 becomes an half line through O_W (denoted by H).

Extremal arcs can be executed by the vehicle in either forward or backward direction: we will hence use superscripts $+$ and $-$ to make this explicit (e.g., S^- stands for a straight line executed backward).

We will build extremal paths consisting of sequences of symbols, or *words*, in the alphabet $\mathcal{A} = \{*, S^+, S^-, E_1^+, E_1^-, E_2^+, E_2^-\}$, where the actual meaning of symbols depends on angles Γ and δ as in fig. 2. Rotations on the spot ($*$) have zero length, but may be used to properly connect other maneuvers.

Let \mathcal{L}_Γ be the set of possible words generated by the aforementioned symbols in \mathcal{A} for each value of Γ . The rest of the paper is dedicated to showing that, due to the physical and geometrical constraints of the considered problem, a sufficient optimal finite language $\mathcal{L}_O \subset \mathcal{L}_\Gamma$

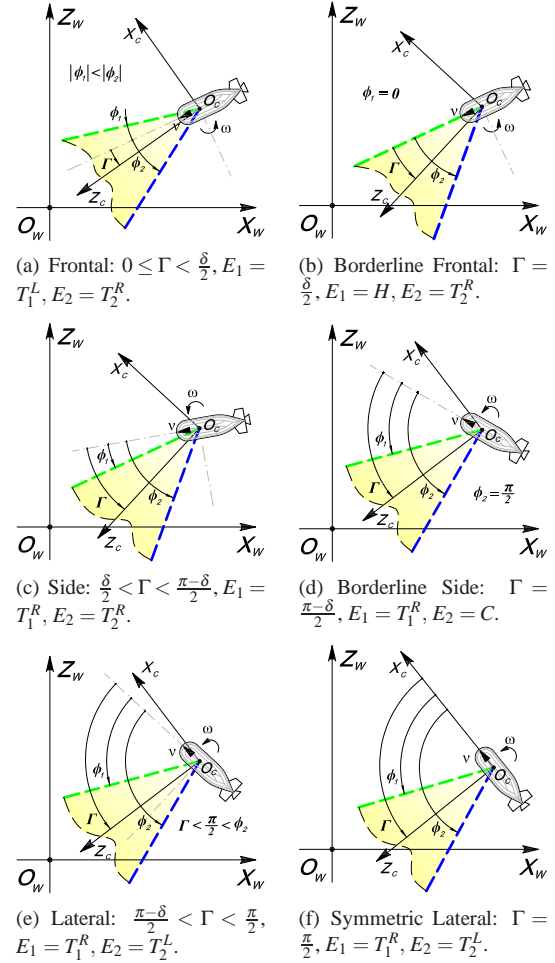


Figure 2: Sensor configuration depending on angles Γ and δ .

can be built such that, for any initial condition, it contains a word describing a path to the goal which is no longer than any other feasible path. Correspondingly, a partition of the plane in a finite number of regions is described, for which the shortest path is one of the words in \mathcal{L}_O .

3 Shortest path synthesis

In this section, we introduce the basic tools that will allow us to study the optimal synthesis of the whole state space

of the robot, beginning from points on a particular subset of \mathbb{R}^2 such that the optimal paths are in a sufficient optimal finite language.

Definition 1. Given the target point $P = (\rho_P, 0)$ in polar coordinates, and $Q \in \mathbb{R}^2 \setminus O_W$, $Q = (\rho_Q, \psi_Q)$ with $\rho_Q \neq 0$, let $f_Q : \mathbb{R}^2 \rightarrow \mathbb{R}^2$ denotes the map

$$f_Q(\rho_G, \psi_G) = \begin{cases} \left(\frac{\rho_G \rho_P}{\rho_Q}, \psi_G - \psi_Q \right) & \text{for } \rho_G \neq 0 \\ (0, 0) & \text{otherwise.} \end{cases} \quad (5)$$

The map f_Q is the combination of a clockwise rotation by angle $\psi_G - \psi_Q$, and a scaling by a factor ρ_P/ρ_Q that maps Q in P .

Remark 1. The alphabet \mathcal{A} is invariant w.r.t. rotation and scaling. However, it is not invariant w.r.t. axial symmetry, as it happened in the particular case (i.e., the Frontal case with $\Gamma = 0$) considered in [13], where the map f_Q was defined as a combination of rotation, scaling and axial symmetry. For example, logarithmic spirals are self-similar and self-congruent (under scaling and rotation they are mapped into themselves). On the other hand, left (right) spirals are mapped into right (left) spirals through an axial symmetry and alphabet invariancy can be lost. Indeed, for example, considering the Side case alphabet (see fig. 2(c)) $\mathcal{A}_{Side} = \{*, S^+, S^-, T_1^{R+}, T_1^{R-}, T_2^{R+}, T_2^{R-}\}$, and applying an axial symmetry we have $T_1^R \rightarrow T_1^L \notin \mathcal{A}_{Side}$, the same occurs for the Frontal alphabet with $\Gamma > 0$.

Let γ be a path parameterized by $t \in [0, 1]$ in the plane of motion $\gamma(t) = (\rho(t), \psi(t))$. Denote with \mathcal{P}_Q the set of all feasible extremal paths from $\gamma(0) = Q$ to $\gamma(1) = P$.

Definition 2. Given the target point $P = (\rho_P, 0)$ and $Q = (\rho_Q, \psi_Q)$ with $\rho_Q \neq 0$, let the path transform function F_Q be defined as

$$F_Q : \mathcal{P}_Q \rightarrow \mathcal{P}_{f_Q(P)} \quad (6)$$

$$\gamma(t) \mapsto f_Q(\gamma(1-t)), \forall t \in I.$$

Notice that $\tilde{\gamma}(t) = F_Q(\gamma(1-t))$ corresponds to $\gamma(t)$ transformed by f_Q and followed in opposite direction. Indeed, $\tilde{\gamma}$ is a path from $\tilde{\gamma}(0) = f_Q(P) = \left(\frac{\rho_P}{\rho_Q}, -\psi_Q\right)$ to $\tilde{\gamma}(1) = f_Q(Q) \equiv P$.

The F map has some properties that make it very useful to the study of our problem in a way which is to some extent similar to what described (for a different F map) in [13]. In particular, the locus of points Q such that $f_Q(P) = Q$, is the circle with center in O_W and radius ρ_P . We will denote this circle by $C(P)$ and the closed disk within $C(P)$ by $D(P)$.

$C(P)$ has an important role in the proposed approach since properties of F_Q will allow us to solve the synthesis problem from points on $C(P)$, and hence to extend the synthesis to $D(P)$ and to the whole motion plane. Indeed, $\forall Q \in C(P)$ and $\forall \gamma \in \mathcal{P}_Q$, $F_Q(\gamma) \in \mathcal{P}_{f_Q(P)}$ with $f_Q(P) \in C(P)$, i.e., a path from a point on $C(P)$ to P is mapped in a path from $C(P)$ to P .

Furthermore, F_Q transforms an extremal in \mathcal{A} in itself but followed in opposite direction. Hence, F_Q maps extremal paths in \mathcal{L}_Γ in extremal paths in \mathcal{L}_Γ . For example, let $w = S^- * H^- * S^+ * T_2^{R+}$ be the word that characterize a path from Q to P , the transformed path is of type $z = T_2^{R-} * S^- * H^+ * S^+$. With a slight abuse of notation, we will write $z = F_Q(w)$.

Proposition 1. Given $Q \in \mathbb{R}^2$ and a path $\gamma \in \mathcal{P}_Q$ of length l , the length of the transformed path $\tilde{\gamma} = F_Q(\gamma)$ is $\tilde{l} = \frac{\rho_P}{\rho_Q} l$.

The proof is easily obtained from a similar result in [13].

Based on the properties of F_Q , optimal paths from points on $C(P)$ completely evolve inside $C(P)$. To prove this statement we first report the following result,

Theorem 1. Given two points $A = (\rho_A, \psi_A)$ and $B = (\rho_B, \psi_B)$, with $\psi_A > \psi_B$ and $\rho = \rho_A = \rho_B$, and an extremal path γ from A to B such that for each point G of γ , $\rho_G > \rho$, there exists an extremal path $\tilde{\gamma}$ from A to B such that for each point \tilde{G} of $\tilde{\gamma}$, $\rho_{\tilde{G}} < \rho$ and $\ell(\tilde{\gamma}) < \ell(\gamma)$ (see fig. 3).

The proof of this theorem can be found in section .1 in the Appendix.

An important but straightforward consequence of the theorem is the following

Corollary 1. For any path in \mathcal{P}_Q with $Q \in C(P)$ there exists a shorter or equal-length path in \mathcal{P}_Q that completely evolves in $D(P)$.

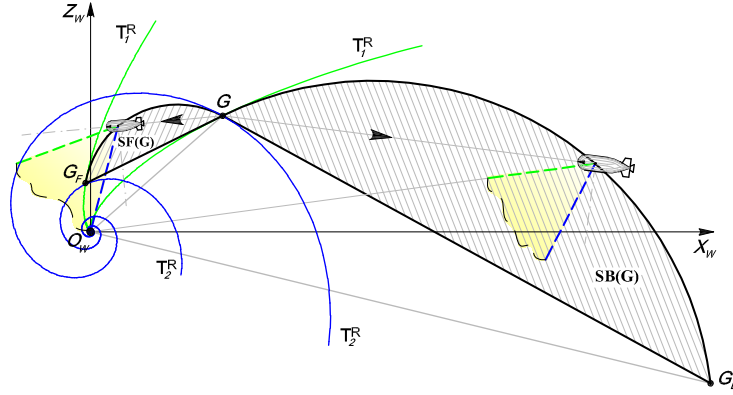


Figure 4: Forward and backward straight path regions from G for $\frac{\delta}{2} < \Gamma \leq \frac{\pi-\delta}{2}$.

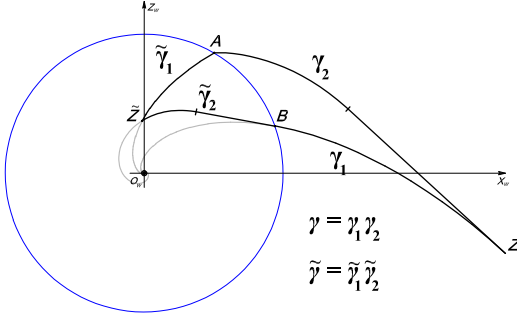


Figure 3: An example for theorem 1: path $\gamma = \gamma_1 \gamma_2$ (γ_1 followed by γ_2) of type $T_2^{R-} S^- * T_1^{R+}$ from A to B is shortened by a path $\tilde{\gamma} = \tilde{\gamma}_1 \tilde{\gamma}_2$ of type $T_1^{R+} * T_1^{R+} S^-$ by applying path transformation F_Z to path γ .

4 Optimal paths for points on $C(P)$

Our study of the optimal synthesis begins in this section addressing optimal paths from points on $C(P)$. We first need to establish an existence result of optimal paths.

Proposition 2. *For any $Q \in C(P)$ there exists a feasible shortest path to P .*

Proof. Because of state constraints (3), and (4), and the restriction of optimal paths in $D(P)$ (Corollary 1) the state set is compact. Furthermore, it is possible to give an upper-bound on the optimal path length for all $\Gamma \in [0, \frac{\pi}{2}]$. Indeed, given a point Q at distance ρ from O_W the optimal

path to P is shorter or equal to the following paths based on the value of Γ and δ :

- Frontal ($0 \leq \Gamma \leq \frac{\delta}{2}$): $S^+ * S^-$ or $H^+ * H^-$ of length $\rho + \rho_P$;
- Side ($\frac{\delta}{2} < \Gamma < \frac{\pi-\delta}{2}$): $T_{1Q}^{R+} * T_{2P}^{R-}$, of length $\left(\frac{\rho - \rho_N}{\cos \phi_1} + \frac{\rho_P - \rho_N}{\cos \phi_2} \right)$, where N is the intersection point between spirals T_{1Q}^R and T_{2P}^R through Q and P respectively;
- Borderline Side ($\Gamma = \frac{\pi-\delta}{2}$): $T_1^{R+} * C_P^-$ of length $\left(\frac{\rho - \rho_P}{\cos \phi_1} + (\psi_N - \psi_P) \rho_P \right)$, where N is the intersection point between spirals T_1^R and C_P ;
- Lateral ($\frac{\pi-\delta}{2} < \Gamma \leq \frac{\pi}{2}$): $T_{2Q}^{L-} * T_{1P}^{R-}$, of length $\left(\frac{\rho - \rho_N}{\cos \phi_2} + \frac{\rho_P - \rho_N}{\cos \phi_1} \right)$, where N is the intersection point between spirals T_{2Q}^L and T_{1P}^R .

The system is also controllable because there always exists an intersection point between two spirals (even if degenerated in half-lines or circumferences) with different characteristic angle even if both clockwise or counter-clockwise around the feature. Hence, Filippov existence theorem for Lagrange problems can be invoked [5]. \square

In the following we provide a set of propositions that completely describe a sufficient optimal finite language for all values of $\Gamma \in [0, \frac{\pi}{2}]$.

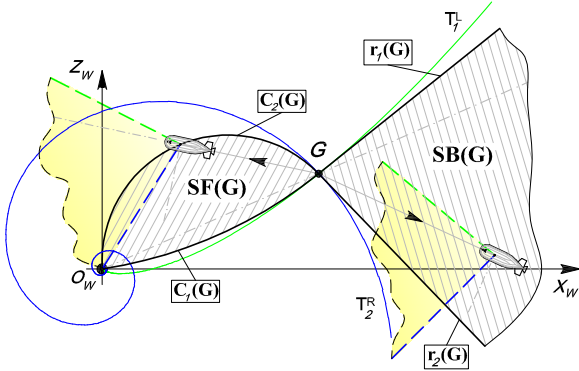


Figure 5: Forward and backward straight path Regions from G for $0 \leq \Gamma \leq \frac{\delta}{2}$.

Definition 3. For any starting point $G = (\rho_G, \psi_G)$, let $SF(G)$ ($SB(G)$) be the set of all points reachable from G with a forward (backward) straight line without violating the SR constraints.

We denote with $\partial SF_1(G)$ and $\partial SF_2(G)$ ($\partial SB_1(G)$ and $\partial SB_2(G)$) the borders of $SF(G)$ ($SB(G)$). Also, let $C_i(G)$ denote the circular arcs from G to O_W such that, $\forall V \in C_i(G)$, $\widehat{GVO_W} = \pi - |\phi_i|$.

Remark 2. Based on simple geometric considerations, for any starting point $G = (\rho_G, \psi_G)$, for $0 \leq \Gamma \leq \frac{\delta}{2}$ (Frontal Case), $SF(G)$ is the region between $\partial SF_2(G) = C_2(G)$ and $\partial SF_1(G) = C_1(G)$. Let $r_1(G)$ ($r_2(G)$) denote the half-line from G forming an angle $\psi_G - \phi_1$ ($\psi_G - \phi_2$) with the X_W axis (cf. fig. 5). $SB(G)$ is the cone delimited by $\partial SB_1(G) = r_1(G)$ and $\partial SB_2(G) = r_2(G)$, outside circle with center in O_W and radius ρ_G . Notice that, $SF(G)$ lays completely in the circle with center in O_W and radius ρ_G . Moreover, in the particular case in which $\Gamma = \frac{\delta}{2}$ (Borderline Frontal Case), $E_1 = H$ and $\partial SF_1(G)$ degenerates in the chord $(\widehat{GO_W})$ between G and O_W , aligned with $r_1(G)$.

As a consequence of Remark 2, both $SF(G)$ and $SB(G)$ are tangent in G to T_1^L or H and T_2^R .

Remark 3. For any starting point $G = (\rho_G, \psi_G)$, and for $\frac{\delta}{2} < \Gamma \leq \frac{\pi - \delta}{2}$ (Side case), let S_{G_F} be the chord between G and $G_F = (\rho_G \frac{\sin \phi_1}{\sin \phi_2}, \psi_G + (\phi_2 - \phi_1)) \in C_2(G)$, i.e. such that $\widehat{O_W G G_F} = \phi_1$ (cf. fig. 4). Naming with C_{G_F} the

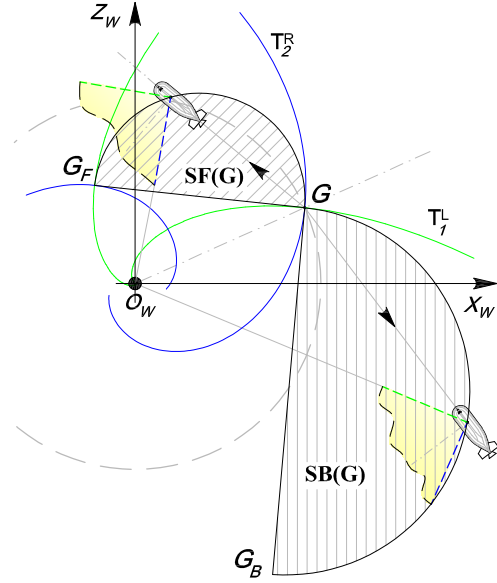


Figure 6: Forward and backward straight path Regions from G for $\frac{\pi - \delta}{2} \leq \Gamma \leq \frac{\pi}{2}$.

arc between G and G_F , $SF(G)$ is the region between arc $\partial SF_2(G) = C_{G_F}$ and chord $\partial SF_1(G) = S_{G_F}$. Consider the rotation and scale that maps G_F in G and G in G_B : we have $\partial SB_1(G) = \partial SF_1(G_B)$, i.e. $\partial SB_2(G) = \partial SF_2(G_B)$. Moreover, for all point V on the circular arc C_{G_B} from G_B to G , angle $\widehat{G_B V O_W} = \pi - |\phi_2|$, and angle $\widehat{O_W G_B G} = \phi_1$. Notice that, in this case, $SF(G)$ lays completely in the circle with center in O_W and radius ρ_G . Notice that, in the particular case in which $\Gamma = \frac{\pi - \delta}{2}$ (Borderline Side Case), $E_2 = C$ and $\partial SF_2(G)$ is an arc from G to G_F on a semi-circle with diameter ρ_G .

As a consequence of Remark 3, $SF(G)$ is tangent in G to T_1^R and T_2^R or C . Moreover, $SF(G)$ is tangent in G_F to T_1^R and T_2^R or C , see fig. 4.

Fig. 6 shows the $SF(G)$ and $SB(G)$ regions described in 3 for the Lateral case. Notice that, in this case, $SF(G)$ does not lay completely in the circle with center in O_W and radius ρ_G .

Remark 4. Optimal forward (backward) straight arcs from any G ends on C_{G_F} (C_{G_B}) (see also [13] for details).

Based on all the above properties, we are now able to

obtain a sufficient family of optimal paths by excluding particular sequences of extremals.

Theorem 2. *Any path consisting in a sequence of a backward extremal arc followed by a forward extremal arc is not optimal.*

The proof of this theorem, whose details can be found in section .2 of the Appendix, is based on the fact that for continuity of paths, for any sequence of a backward extremal followed by a forward one, there exist points A and B that verify hypothesis of Theorem 1.

Theorem 3. *Any path consisting in a sequence of an extremal arc E_i and an extremal arc E_j followed in the same direction is not optimal for any $i, j \in \{1, 2\}$ with $i \neq j$.*

Notice that the feasible sequences consisting of two extremals that we still need to discuss are those starting or ending with S followed in any direction (E^+E^- and E^-E^+ are obviously not optimal).

Proposition 3. *From any starting point A , any path γ of type $S^+ * E_2^+$ and $S^+ * E_1^-$ to B can be shortened by a path of type $S^+E_2^+$ or $E_2^+ * E_1^-$. Moreover, any path γ of type $S^+ * E_1^+$ or $S^+ * E_2^-$ can be shortened by a path of type $E_1^+S^+$ or $E_1^+ * E_2^-$.*

Proposition 3 implies that paths of type $S^- * E_1^-$ and $S^- * E_2^-$ are not optimal. Indeed, they can be shortened by $S^-E_1^-$ and $E_2^-S^-$, respectively (see fig. 7 for the Side case).

By using all previous results, a sufficient family of optimal paths is obtained in the following important theorem.

Theorem 4. *For $\frac{\delta}{2} < \Gamma \leq \frac{\pi}{2}$, i.e. Side and Lateral cases, and for any $Q \in D(P)$ to P there exists a shortest path of type $E_1^+ * E_2^-S^-E_1^-$ or of type $E_1^+S^+E_2^+ * E_1^-$. For $0 \leq \Gamma \leq \frac{\delta}{2}$, i.e. Frontal case, and for any $Q \in D(P)$ to P there exists a shortest path of type $S^+E_1^+ * E_2^-S^-$ or of type $S^+E_2^+ * E_1^-S^-$.*

Proof. According to all propositions above several concatenations of extremal have been proved to be non optimal. Considering extremals as node and, possibly optimal, concatenations of extremal as edges of a graph, the sufficient optimal languages \mathcal{L}_O from Q in $D(P)$, for different values of Γ and δ , are described in fig. 8. Indeed, it is straightforward to observe that the number of switches

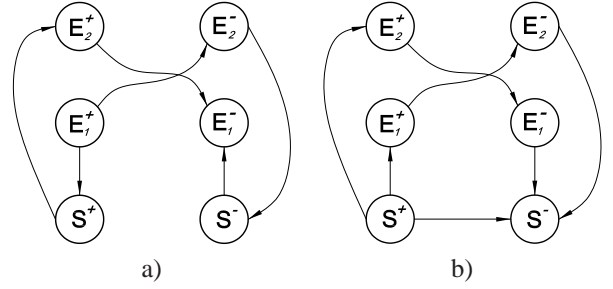


Figure 8: Feasible extremals and sequence of extremals from point in $D(P)$: a) in Side and Lateral cases ($\frac{\delta}{2} < \Gamma \leq \frac{\pi}{2}$). b) in Frontal case ($0 \leq \Gamma \leq \frac{\delta}{2}$).

between extremals is finite and less or equal to 3, for any value of Γ and δ . Hence, the thesis. \square

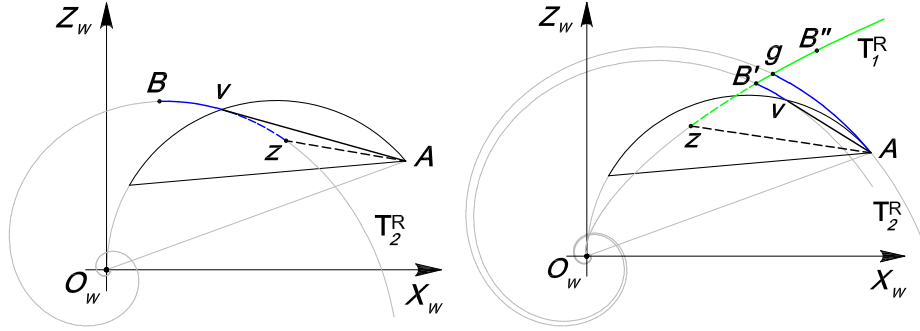
We now study the length of extremal paths from $C(P)$ to P in the sufficient family above.

Without loss of generality, it is sufficient to study the length of extremal paths of type $E_1^+ * E_2^-S^-E_1^-$ only from points Q on the semicircle of $C(P)$ in the upper-half plane (denoted by CS). Indeed, up to a rotation, optimal paths of type $E_1^+S^+E_2^+ * E_1^-$ from the rest of $C(P)$ can be easily obtained. Referring to fig. 9, let the switching points of the optimal path be denoted by N , M_1 and M_2 or \bar{N} , \bar{M}_1 and $\bar{M}_2 \equiv P$, respectively, depending on the angular values α_{M_1} or $\alpha_{\bar{M}_1}$. Moreover, in order to do the analysis, it is useful to parameterize the family by the angular value $\alpha_{\bar{M}_1}$ of the switching point \bar{M}_1 along the arc $C_2(P)$ between P and Z or the angular value α_{M_1} of the switching point M_1 along the extremal E_1 between P_F and O_W .

Theorem 5. *For any point $Q \in CS$, the length of a path $\gamma \in \mathcal{P}_Q$ of type $E_1^+ * E_2^-S^-E_1^-$ is:*

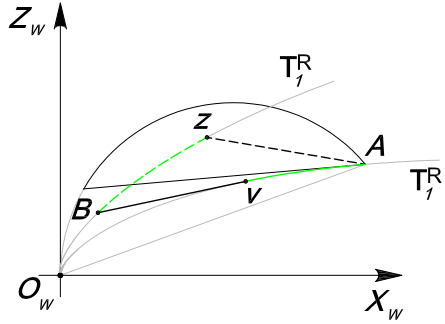
- for $0 \leq \alpha_{\bar{M}_1} \leq \phi_2 - \phi_1$, i.e. from P to Z (notice that the last arc has zero length):

$$L = \rho_P \left\{ \frac{\cos \alpha_{M_1}}{\cos \phi_2} + \frac{1}{\cos \phi_1} + \frac{\cos \phi_1 + \cos \phi_2}{\cos \phi_1 \cos \phi_2} e^{(\psi_Q - \alpha_{M_1}) \frac{r_1 r_2}{r_2 - r_1}} \left(\frac{\sin(\phi_2 - \alpha_{M_1})}{\sin \phi_2} \right)^{-\frac{r_1}{r_2 - r_1}} \right\}, \quad (7)$$

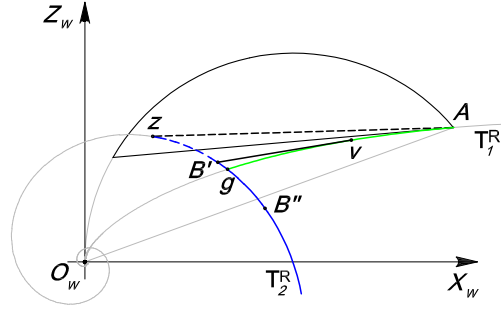


(a) From A to B, path $S^+ * T_2^{R+}$ through z and v can be shortened by $S^+ T_2^{R+}$ through v, where S arc is tangent to T_2^R .

(b) From A to B', path $S^+ * T_1^{R-}$ through z can be shortened by a path of type $S^+ T_2^{R+}$ through v, whereas from A to B'' by a path of type $T_2^{R+} * T_1^{R-}$ through g.



(c) From A to B, path $S^+ * T_1^{R+}$ through z can be shortened by a path of type $T_1^{R+} S^+$ through v, where S arc is tangent to T_1^R .



(d) From A to B', path $S^+ * T_2^{R-}$ through z can be shortened by a path of type $T_1^{R+} S^+$ through v, whereas from A to B'' by a path of type $T_1^{R+} * T_2^{R-}$ through g.

Figure 7: Examples of paths shortened in proposition 3 for the Side case.

- for $\alpha_{M_1} \geq \phi_2 - \phi_1$, i.e. from Z to O_W :

$$L = \rho_P \left\{ \frac{2}{\cos \phi_1} + e^{-\alpha_{M_1} t_1} \left[\frac{\cos(\phi_2 - \phi_1)}{\cos \phi_2} - \frac{1}{\cos \phi_1} + \frac{-\cos \phi_1 + \cos \phi_2}{\cos \phi_1 \cos \phi_2} e^{[\psi_Q - (\phi_2 - \phi_1)] \frac{t_1 t_2}{t_2 - t_1}} \left(\frac{\sin \phi_1}{\sin \phi_2} \right)^{-\frac{t_1}{t_2 - t_1}} \right] \right\}, \quad (8)$$

with $t_1 = 1/\tan \phi_1$ and $t_2 = 1/\tan \phi_2$.

The analytical expression for the length L is based on a direct computation. Having the path's length as a function of two parameters α_{M_1} or $\alpha_{\bar{M}_1}$ and ψ_Q , we are now in a position to minimize the length within the sufficient family.

Theorem 6. Given a point $Q \in CS$,

- for $0 \leq \psi_Q \leq \psi_{R_1} := \frac{\sin(\phi_2 - \phi_1)}{\cos \phi_1 \cos \phi_2} \ln \left(\frac{\cos \phi_1 + \cos \phi_2}{\sin \phi_2 \sin(\phi_2 - \phi_1)} \right)$, optimal path is of type $E_1^+ * E_2^-$;
- for $\psi_{R_1} \leq \psi_Q \leq \psi_{R_2}$ with $\psi_{R_2} := (\phi_2 - \phi_1) + \psi_{R_1} + \tan \phi_2 \ln \left(\frac{\sin \phi_1}{\sin \phi_2} \right)$, optimal path is of type $E_1^+ * E_2^- S^-$;
- for $\psi_{R_2} \leq \psi_Q \leq \pi$ the optimal path is $E_1^+ * E_1^-$ through O_W .

Moreover, for $\psi_Q = \psi_{R_2}$, any optimal path of type $E_1^+ * E_2^- S^- E_1^-$ turns out to have the same length ℓ of optimal path $E_1^+ * E_1^-$. Hence, for $\psi_Q = \psi_{R_2}$ also $E_1^+ * E_2^- S^- E_1^-$ is optimal.

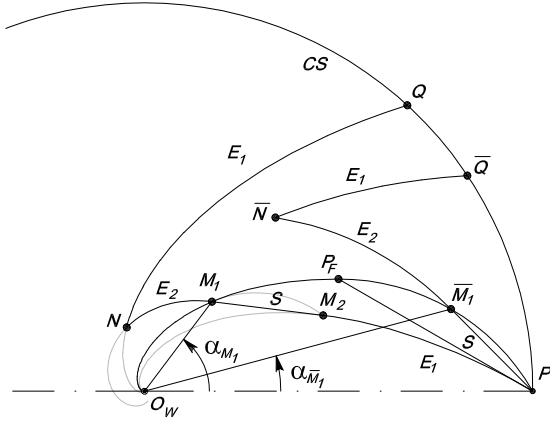


Figure 9: Path of type $E_1^+ * E_2^- S^- E_1^-$ or the degenerate case of type $E_1^+ * E_2^- S^-$ from $Q \in CS$.

Previous results have been obtained computing first and second derivatives of L and nonlinear minimization techniques.

We are now interested in determining the locus of switching points between extremals in optimal paths.

Proposition 4. For $Q \in CS$ with $0 < \psi_Q \leq \psi_{R_1}$, the switching locus is the arc of E_2 between P $M = (\rho_P \frac{\sin \phi_2 \sin(\phi_2 - \phi_1)}{\cos \phi_1 + \cos \phi_2}, \psi_M)$ (included), where $\psi_M = \tan \phi_2 \ln \left(\frac{\rho_P}{\rho_M} \right)$.

Proof. From Theorem 6, the optimal path from $Q \in CS$ to P is of type $E_1^+ * E_2^-$. For $\psi_Q = \psi_{R_1}$ the intersection between E_1^+ and E_2^- is M . \square

Proposition 5. For $Q \in CS$ with $\psi_{R_1} < \psi_Q < \psi_{R_2}$, the loci of switching points M_2 and N are the $\partial SF_2(P)$ and $\partial SF_2(M)$.

Proof. For $Q \in CS$ with $\psi_{R_1} < \psi_Q < \psi_{R_2}$, considering the values of α_{M_2} obtained in the computations of Theorem 6 we obtain $M_2 \in \partial SF_2(P)$. Furthermore, substituting those values in the equation of the intersection point N between E_1 through Q and E_2 through M_2 we obtain $N \in \partial SF_2(M)$. \square

Finally, for $Q \in CS$ with $\psi_{R_2} \leq \psi < \pi$, the switching locus reduces to the origin O_W since two extremal E_i intersect only in the origin for $i = 1, 2$.

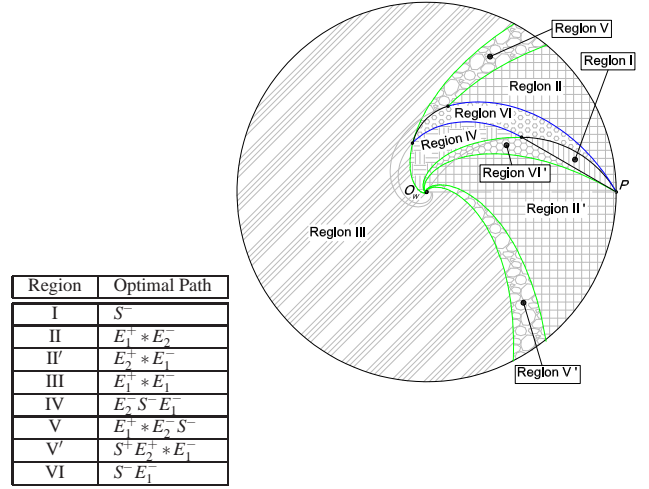


Figure 10: Optimal synthesis inside $D(P)$.

5 Shortest paths from any point in the motion plane

The synthesis on $C(P)$ induce a partition in regions of $D(P)$. Indeed, for any $Q \in D(P)$, there exists a point $V \in C(P)$ such that the optimal path γ from V to P goes through Q . The Bellmann's optimality principle ensure the optimality of the sub-path from Q to P . Based on this construction the partition of $C(P)$ is reported in fig. 10.

For points outside $C(P)$, function F_Q has been defined in 6 in order to transform paths starting from Q inside $C(P)$ in paths starting from $f_Q(P) = \left(\frac{\rho_P^2}{\rho_Q}, -\psi_Q \right)$ outside $C(P)$.

From other properties of F_Q , such as Proposition 1, we have also that an optimal path is mapped into an optimal path. Hence, the optimal synthesis from points outside $C(P)$ can be easily obtained mapping through map F_Q all borders of regions inside $C(P)$.

Proposition 6. Given a border \mathbf{B} and $Q \in \mathbf{B}$ map F_Q transforms:

1. $\mathbf{B} = C(P)$ into itself;
2. $\mathbf{B} = \partial SF_2(Q)$ in $\partial SB_1(f_Q(P))$
3. $\mathbf{B} = \partial SF_1(Q)$ in $\partial SB_2(f_Q(P))$

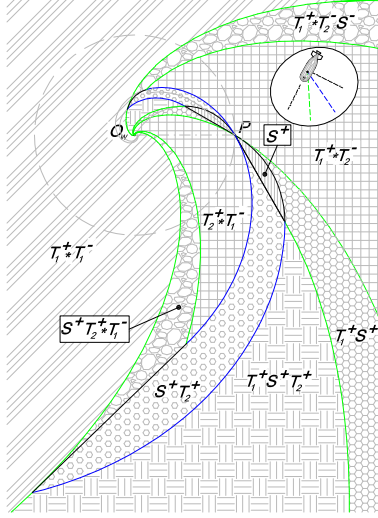


Figure 11: Partition of the motion plane for $\frac{\delta}{2} < \Gamma < \frac{\pi-\delta}{2}$.

4. $\mathbf{B} = E_i$ in arcs of the same type ($i = 1, 2$)

Proof. The proof of this proposition can be found in [13]. \square

Based on Proposition 6, the optimal synthesis of the entire motion plane is reported in fig. 11.

6 Optimal synthesis for generic Γ

We first obtain the synthesis of the Borderline Frontal case, i.e. $\Gamma = \frac{\delta}{2}$, reported in fig. 12 from the one obtained in the previous section.

Notice that, $E_1 = T_1^R$ of the Side case degenerates in a straight line H through O_W for $\Gamma = \frac{\delta}{2}$. Indeed, referring to fig. 10, points M_F and P_F degenerate on O_W . As a consequence, Region IV, IV and VI' while coordinates Ψ_{R_1} and Ψ_{R_2} of points R_1 and R_2 can be obtained from values in 6 replacing $\phi_1 = 0$.

In the Frontal case, $E_1 = H$ becomes a spiral T_1^L , straight lines from P and R_2 split in straight line and a spiral arc generating the partition reported in fig. 13. In this case, $\phi_1 < 0$ and points R_1 and R_2 do not lay on $C(P)$ but on a circle through P with center $(0, -\rho_P \frac{\sin^2 \phi_1 - \sin^2 \phi_2}{2 \sin \xi \sin \phi_1 \sin \phi_2})$, where $\xi =$

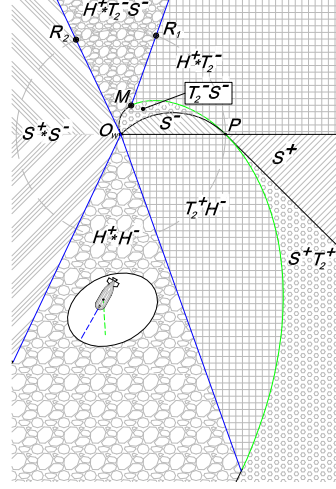


Figure 12: Partition of the motion plane for $\Gamma = \delta/2$ (i.e. a SR border is aligned with the robot motion direction, Borderline Frontal).

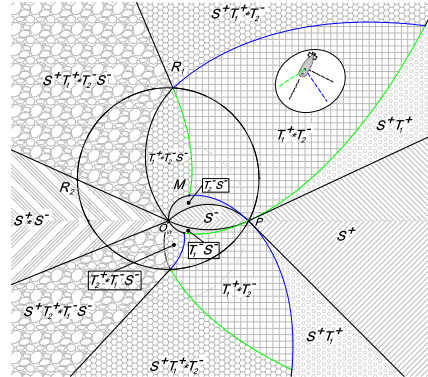


Figure 13: Partition of the motion plane for $0 \leq \Gamma < \frac{\delta}{2}$, i.e. Frontal case.

$\frac{l_1+l_2}{l_1 l_2} \ln \left(\frac{\cos \phi_1 + \cos \phi_2}{\sin(\phi_2 - \phi_1)} \right) + \frac{1}{l_1} \ln(-\sin \phi_1) - \frac{1}{l_2} \ln(\sin \phi_2)$. Notice that for $\phi_2 = -\phi_1$, this circle coincide with $C(P)$ and the synthesis proposed in [13] is obtained.

Referring again to fig. 10, in the Borderline Side case ($\Gamma = \frac{\pi-\delta}{2}$, i.e. the SR border is aligned with the axle direction and $\phi_2 = \frac{\pi}{2}$), $E_2 = T_2^R$ degenerates in $E_2 = C$. Points $R_1 \equiv M$ and R_2 lays on $C(P)$ with $\Psi_{R_1} = \frac{1+\sin \phi_1}{\cos \phi_1}$ and $\Psi_{R_2} = \frac{\pi}{2} - \phi_1 + \Psi_{R_1} + \tan \phi_1 \ln(\sin \phi_1)$. The obtained

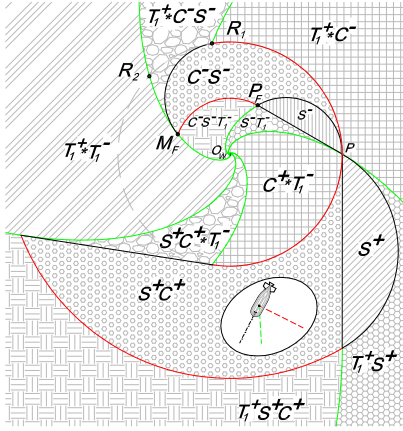


Figure 14: Partition of the motion plane for $\Gamma = \frac{\pi-\delta}{2}$ (i.e. a SR border is aligned with the axle direction).

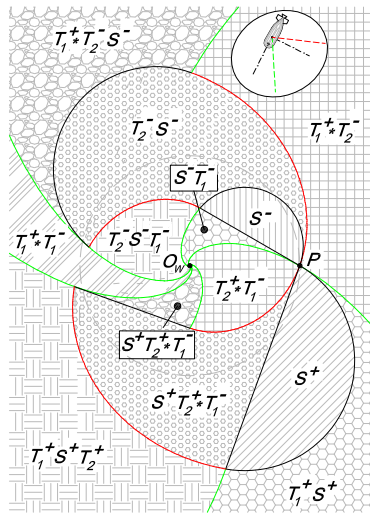


Figure 15: Partition of the motion plane for $\frac{\pi-\delta}{2} \leq \Gamma < \frac{\pi}{2}$ (i.e. axle direction is included inside the SR).

synthesis is reported in fig. 14. For the Lateral case $E_2 = C$ becomes $E_2 = T_2^L$ and the synthesis of the Lateral case, reported in fig. 15, can be obtained from the one in fig. 14.

The subdivision of the motion plane in case of $\frac{\pi}{2} < \Gamma \leq \pi$ can be easily obtained by using that one for $0 \leq \Gamma \leq \frac{\pi}{2}$ considering optimal path followed in reverse order, i.e. forward arc in backward arc and viceversa. Finally, a

symmetry w.r.t. X_W axis of each subdivision of the motion plane for each $\Gamma \in [0, \pi]$ allows to obtain the corresponding subdivision for $\Gamma \in [-\pi, 0]$.

7 Conclusions and future work

A complete characterization of shortest paths for unicycle nonholonomic mobile robots equipped with a limited range side sensor systems has been proposed. A finite sufficient family of optimal paths has been determined based on geometrical properties of the considered problem. Finally, a complete shortest path synthesis to reach a point keeping a feature in sight has been provided. A possible extension of this work is to consider a bounded 3D SR pointing to any direction with respect to the direction of motion. A more challenging extension would be considering a different minimization problem such as the minimum time.

References

- [1] D. Balkcom and M. Mason. Time-optimal trajectories for an omnidirectional vehicle. *The International Journal of Robotics Research*, 25(10):985–999, 2006.
- [2] S. Bhattacharya, R. Murrieta-Cid, and S. Hutchinson. Optimal paths for landmark-based navigation by differential-drive vehicles with field-of-view constraints. *IEEE Transactions on Robotics*, 23(1):47–59, February 2007.
- [3] A.E. Bryson and Y.C. Ho. *Applied optimal control*. Wiley New York, 1975.
- [4] X.N. Bui, P. Souères, J-D. Boissonnat, and J-P. Laumond. Shortest path synthesis for Dubins non-holonomic robots. In *IEEE International Conference on Robotics and Automation*, pages 2–7, 1994.
- [5] L. Cesari. *Optimization-theory and applications: problems with ordinary differential equations*. Springer-Verlag, New York, 1983.
- [6] H. Chitsaz, S. M. LaValle, D. J. Balkcom, and M.T. Mason. Minimum wheel-rotation for differential-

drive mobile robots. *The International Journal of Robotics Research*, pages 66–80, 2009.

- [7] M. Chyba, N.E. Leonard, and E.D. Sontag. Optimality for underwater vehicle's. In *40th IEEE Conference on Decision and Control*, volume 5, pages 4204–4209, 2001.
- [8] N. Dias, C. Almeida, H. Ferreira, J. Almeida, A. Martins, A. Dias, and E. Silva. Manoeuvre based mission control system for autonomos surface vehicle. in *Proceedings of OCEANS '09*, May 2009.
- [9] L. E. Dubins. On curves of minimal length with a constraint on average curvature, and with prescribed initial and terminal positions and tangents. *American Journal of Mathematics*, pages 457–516, 1957.
- [10] F. Langner, C. Knauer, W. Jans, and A. Ebert. Side scan sonar image resolution and automatic object detection, classification and identification. in *Proceedings of OCEANS '09*, May 2009.
- [11] J. A. Reeds and L. A. Shepp. Optimal paths for a car that goes both forwards and backwards. *Pacific Journal of Mathematics*, pages 367–393, 1990.
- [12] P. Salaris, D. Fontanelli, L. Pallottino, and A. Bicchi. Optimal paths for mobile robots with limited field of view camera. In *48th IEEE Conference on Decision and Control*, pages 8434–8439, Dec 2009.
- [13] P. Salaris, D. Fontanelli, L. Pallottino, and A. Bicchi. Shortest paths for a robot with nonholonomic and field-of-view constraints. *IEEE Transactions on Robotics*, 26(2):269–281, April 2010.
- [14] H. Souères and J. P. Laumond. Shortest paths synthesis for a car-like robot. *IEEE Transaction on Automatic Control*, pages 672–688, 1996.
- [15] H. Sussmann and G. Tang. Shortest paths for the reeds-shepp car: A worked out example of the use of geometric techniques in nonlinear optimal control. Technical report, Department of Mathematics, Rutgers University, 1991.
- [16] H. Wang, Y. Chan, and P. Souères. A geometric algorithm to compute time-optimal trajectories for

a bidirectional steered robot. *IEEE Transaction on Robotics*, pages –, 2009.

.1 Proof of Theorem 1

Theorem 1. *Given two points $A = (\rho_A, \psi_A)$ and $B = (\rho_B, \psi_B)$, with $\psi_A > \psi_B$ and $\rho = \rho_A = \rho_B$, and an extremal path γ from A to B such that for each point G of γ , $\rho_G > \rho$, there exists an extremal path $\tilde{\gamma}$ from A to B such that for each point \tilde{G} of $\tilde{\gamma}$, $\rho_{\tilde{G}} < \rho$ and $\ell(\tilde{\gamma}) < \ell(\gamma)$.*

Proof. Consider a point $Z = (\rho_Z, \psi_Z)$ such that $\rho_Z = \max_{G \in \gamma} \rho_G > \rho$. Let γ_1 and γ_2 the sub-paths of γ from Z to B and from Z to A .

The sub-path γ_1 , is rotated and scaled (contracted of factor $\frac{\rho}{\rho_Z} < 1$) such that Z is transformed in A obtaining a path $\tilde{\gamma}_1$ from A to $\tilde{Z} = (\frac{\rho^2}{\rho_Z}, \psi_A + \psi_B - \psi_Z)$. Similarly, γ_2 , can be rotated and scaled with the same scale factor but different rotation angle w.r.t. γ_1 such that Z is transformed in B , see fig. 3. After geometrical considerations, it is easy to notice that the obtained path $\tilde{\gamma}_2$ starts in B and ends in \tilde{Z} .

The obtained paths are a contraction of γ_1 and γ_2 respectively and hence shorter. Moreover, any point G of γ_1 or γ_2 has $\rho_G > \rho$ hence is scaled in \tilde{G} of $\tilde{\gamma}_1$ or $\tilde{\gamma}_2$ with $\rho_{\tilde{G}} = \frac{\rho \rho_G}{\rho_Z} < \rho$.

Concluding, we have obtained a shorter path from A to B that evolves completely in the disk of radius ρ . \square

.2 Proof of Theorem 2

Theorem 2. *Any path consisting in a sequence of a backward extremal arc followed by a forward extremal arc is not optimal.*

Proof. Observe that the distance from O_W is strictly increasing along backward extremal arcs (i.e. S^-, E_1^-, E_2^- with $E_2 \neq C$) and strictly decreasing along forward extremal arcs (i.e. S^+, E_1^+, E_2^+ with $E_2 \neq C$). For continuity of paths, for any sequence of a backward extremal followed by a forward one, there exist points A and B that verify hypothesis of Theorem 1, hence it is not optimal.

Any sequence consisting in an extremal S (or E_1) of length ℓ and an extremal $E_2 = C$ (in any order and direction) is inscribed in two circumferences centered in O_W . Hence, the shortest sequence is the one with $E_2 = C$ along

the circle of smaller radius necessarily preceded by a forward S (or E_1) of same length ℓ .

Concluding, in an optimal path a forward arc cannot follow a backward arc. \square